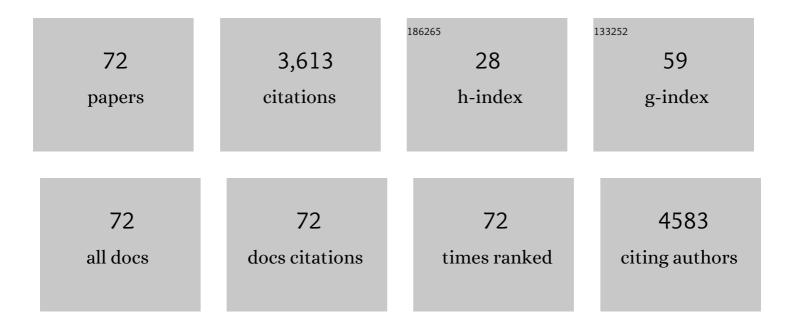
Lijuan Zhang

List of Publications by Year in descending order

Source: https://exaly.com/author-pdf/2312585/publications.pdf Version: 2024-02-01



#	Article	IF	CITATIONS
1	Controllable formation of bulk perfluorohexane nanodroplets by solvent exchange. Soft Matter, 2022, 18, 425-433.	2.7	1
2	Influence of the Dissolved Gas on the Interfacial Properties of Decane Surface Nanodroplets. Langmuir, 2022, 38, 2213-2219.	3.5	4
3	Theoretical Analysis on the Stability of Single Bulk Nanobubble. Frontiers in Materials, 2022, 9, .	2.4	3
4	Editorial: Particle Interfaces & amp; Interface Performance Materials. Frontiers in Materials, 2022, 9, .	2.4	0
5	Gram-selective antibacterial peptide hydrogels. Biomaterials Science, 2022, 10, 3831-3844.	5.4	10
6	Interfacial Micropancakes: Gas or Contaminations?. Langmuir, 2022, 38, 7914-7920.	3.5	7
7	Generating Bulk Nanobubbles in Alcohol Systems. ACS Omega, 2021, 6, 2873-2881.	3.5	5
8	Antimicrobial <scp>d</scp> -Peptide Hydrogels. ACS Biomaterials Science and Engineering, 2021, 7, 1703-1712.	5.2	22
9	Macrochirality of Self-Assembled and Co-assembled Supramolecular Structures of a Pair of Enantiomeric Peptides. Frontiers in Molecular Biosciences, 2021, 8, 700964.	3.5	5
10	Collective Dynamics of Bulk Nanobubbles with Size-Dependent Surface Tension. Langmuir, 2021, 37, 7986-7994.	3.5	16
11	Generation and stability of bulk nanobubbles: A review and perspective. Current Opinion in Colloid and Interface Science, 2021, 53, 101439.	7.4	69
12	Three-dimensional ultrastructural imaging reveals the nanoscale architecture of mammalian cells. Microscopy and Microanalysis, 2021, 27, 1566-1569.	0.4	0
13	Gelation of a Pentapeptide in Alcohols. Langmuir, 2021, 37, 8961-8970.	3.5	3
14	The effects of nanobubbles on the assembly of glucagon amyloid fibrils. Soft Matter, 2021, 17, 3486-3493.	2.7	5
15	3D Imaging and Quantification of the Integrin at a Single-Cell Base on a Multisignal Nanoprobe and Synchrotron Radiation Soft X-ray Tomography Microscopy. Analytical Chemistry, 2021, 93, 1237-1241.	6.5	20
16	Novel 2D CaCl crystals with metallicity, room-temperature ferromagnetism, heterojunction, piezoelectricity-like property and monovalent calcium ions. National Science Review, 2021, 8, nwaa274.	9.5	16
17	Wetting Behavior of Surface Nanodroplets Regulated by Periodic Nanostructured Surfaces. ACS Applied Materials & Interfaces, 2021, 13, 55726-55734.	8.0	7
18	Single-Particle Analysis for Structure and Iron Chemistry of Atmospheric Particulate Matter. Analytical Chemistry, 2020, 92, 975-982.	6.5	24

Lijuan Zhang

#	Article	IF	CITATIONS
19	Influence of Krypton Gas Nanobubbles on the Activity of Pepsin. Langmuir, 2020, 36, 14070-14075.	3.5	11
20	The effect of oxygen vacancy and spinel phase integration on both anionic and cationic redox in Li-rich cathode materials. Journal of Materials Chemistry A, 2020, 8, 7733-7745.	10.3	101
21	Formation and Stability of Bulk Nanobubbles by Vibration. Langmuir, 2020, 36, 2264-2270.	3.5	47
22	Ultrahigh Density of Gas Molecules Confined in Surface Nanobubbles in Ambient Water. Journal of the American Chemical Society, 2020, 142, 5583-5593.	13.7	88
23	Oxygenation and synchronous control of nitrogen and phosphorus release at the sediment-water interface using oxygen nano-bubble modified material. Science of the Total Environment, 2020, 725, 138258.	8.0	33
24	Pyrolysis Temperature-Dependent Changes in the Characteristics of Biochar-Borne Dissolved Organic Matter and Its Copper Binding Properties. Bulletin of Environmental Contamination and Toxicology, 2019, 103, 169-174.	2.7	53
25	Effect of Sodium Oleate on the Adsorption Morphology and Mechanism of Nanobubbles on the Mica Surface. Langmuir, 2019, 35, 9239-9245.	3.5	40
26	Lithiumâ€Ion Batteries: Tuning Anionic Redox Activity and Reversibility for a Highâ€Capacity Liâ€Rich Mnâ€Based Oxide Cathode via an Integrated Strategy (Adv. Funct. Mater. 10/2019). Advanced Functional Materials, 2019, 29, 1970064.	14.9	7
27	Formation and Stability of Bulk Nanobubbles in Different Solutions. Langmuir, 2019, 35, 5250-5256.	3.5	58
28	Mechanical Properties of Sub-Microbubbles with a Nanoparticle-Decorated Polymer Shell. Langmuir, 2019, 35, 17090-17095.	3.5	4
29	Force Spectroscopy Revealed a High-Gas-Density State near the Graphite Substrate inside Surface Nanobubbles. Langmuir, 2019, 35, 2498-2505.	3.5	26
30	Tuning Anionic Redox Activity and Reversibility for a Highâ€Capacity Liâ€Rich Mnâ€Based Oxide Cathode via an Integrated Strategy. Advanced Functional Materials, 2019, 29, 1806706.	14.9	121
31	Influence of Mixing and Nanosolids on the Formation of Nanobubbles. Journal of Physical Chemistry B, 2019, 123, 317-323.	2.6	23
32	The role of EDTA on rutile flotation using Al ³⁺ ions as an activator. RSC Advances, 2018, 8, 4872-4880.	3.6	18
33	Structural Incorporation of Manganese into Goethite and Its Enhancement of Pb(II) Adsorption. Environmental Science & Technology, 2018, 52, 4719-4727.	10.0	74
34	Changes in structural characteristics and metal speciation for biochar exposure in typic udic ferrisols. Environmental Science and Pollution Research, 2018, 25, 153-162.	5.3	8
35	3D Heterogeneous Co ₃ O ₄ @Co ₃ S ₄ Nanoarrays Grown on Ni Foam as a Binderâ€Free Electrode for Lithiumâ€Ion Batteries. ChemElectroChem, 2018, 5, 309-315.	3.4	35
36	Automatic Calibrations of Sample Misalignment for Nanotomography at SSRF. Microscopy and Microanalysis, 2018, 24, 124-125.	0.4	1

LIJUAN ZHANG

#	Article	IF	CITATIONS
37	Formation and Stability of Surface/Bulk Nanobubbles Produced by Decompression at Lower Gas Concentration. Journal of Physical Chemistry C, 2018, 122, 22418-22423.	3.1	42
38	The Role of Nanobubbles in the Precipitation and Recovery of Organic-Phosphine-Containing Beneficiation Wastewater. Langmuir, 2018, 34, 6217-6224.	3.5	54
39	CH ₄ Nanobubbles on the Hydrophobic Solid–Water Interface Serving as the Nucleation Sites of Methane Hydrate. Langmuir, 2018, 34, 10181-10186.	3.5	48
40	Three-dimensional ultrastructural imaging reveals the nanoscale architecture of mammalian cells. IUCrJ, 2018, 5, 141-149.	2.2	24
41	Formation and Stability of Bulk Nanobubbles Generated by Ethanol–Water Exchange. ChemPhysChem, 2017, 18, 1345-1350.	2.1	89
42	lon sieving in graphene oxide membranes via cationic control of interlayer spacing. Nature, 2017, 550, 380-383.	27.8	1,171
43	Inert Gas Deactivates Protein Activity by Aggregation. Scientific Reports, 2017, 7, 10176.	3.3	25
44	Interfacial gas nanobubbles or oil nanodroplets?. Physical Chemistry Chemical Physics, 2017, 19, 1108-1114.	2.8	26
45	Formation of surface nanobubbles on nanostructured substrates. Nanoscale, 2017, 9, 1078-1086.	5.6	44
46	Unexpectedly Enhanced Solubility of Aromatic Amino Acids and Peptides in an Aqueous Solution of Divalent Transition-Metal Cations. Physical Review Letters, 2016, 117, 238102.	7.8	41
47	Rhodamine B-based ordered mesoporous organosilicas for the selective detection and adsorption of Al(<scp>iii</scp>). New Journal of Chemistry, 2016, 40, 6752-6761.	2.8	11
48	Enhanced Fluorescence in Tetraylnitrilomethylidyne–Hexaphenyl Derivative-Functionalized Periodic Mesoporous Organosilicas for Sensitive Detection of Copper(II). Journal of Physical Chemistry C, 2016, 120, 9299-9307.	3.1	30
49	Size-Dependent Stiffness of Nanodroplets: A Quantitative Analysis of the Interaction between an AFM Probe and Nanodroplets. Langmuir, 2016, 32, 11230-11235.	3.5	10
50	Solid-solution partitioning and thionation of diphenylarsinic acid in a flooded soil under the impact of sulfate and iron reduction. Science of the Total Environment, 2016, 569-570, 1579-1586.	8.0	8
51	Metal-enhanced fluorescence-based multilayer core–shell Ag-nanocube@SiO ₂ @PMOs nanocomposite sensor for Cu ²⁺ detection. RSC Advances, 2016, 6, 61109-61118.	3.6	16
52	Influence of water-dispersible colloids from organic manure on the mechanism of metal transport in historically contaminated soils: coupling colloid fractionation with high-energy synchrotron analysis. Journal of Soils and Sediments, 2016, 16, 349-359.	3.0	6
53	In situ measurement of contact angles and surface tensions of interfacial nanobubbles in ethanol aqueous solutions. Soft Matter, 2016, 12, 3303-3309.	2.7	30
54	Distribution and Speciation of Cu in the Root Border Cells of Rice by STXM Combined with NEXAFS. Bulletin of Environmental Contamination and Toxicology, 2016, 96, 408-414.	2.7	7

Lijuan Zhang

#	Article	IF	CITATIONS
55	Interfacial Nanobubbles on Atomically Flat Substrates with Different Hydrophobicities. ChemPhysChem, 2015, 16, 1003-1007.	2.1	26
56	X-Ray Absorption Spectra and Self-Bias Ferromagnetic Resonance of FeCoB Films Prepared by Composition Gradient Sputtering. IEEE Transactions on Magnetics, 2015, 51, 1-4.	2.1	2
57	Stiffness and evolution of interfacial micropancakes revealed by AFM quantitative nanomechanical imaging. Physical Chemistry Chemical Physics, 2015, 17, 13598-13605.	2.8	24
58	Where Does the Transformation of Precipitated Ceria Nanoparticles in Hydroponic Plants Take Place?. Environmental Science & Technology, 2015, 49, 10667-10674.	10.0	82
59	The Origin of the "Snapâ€inâ€in the Force Curve between AFM Probe and the Water/Gas Interface of Nanobubbles. ChemPhysChem, 2014, 15, 492-499.	2.1	17
60	Selective synthesis of clinoatacamite Cu2(OH)3Cl and tenorite CuO nanoparticles by pH control. Journal of Nanoparticle Research, 2014, 16, 1.	1.9	28
61	Metallofullerenols: Polyhydroxylated Metallofullerenols Stimulate IL-1β Secretion of Macrophage through TLRs/MyD88/NF-κB Pathway and NLRP3Inflammasome Activation (Small 12/2014). Small, 2014, 10, 2310-2310.	10.0	2
62	Mechanical mapping of nanobubbles by PeakForce atomic force microscopy. Soft Matter, 2013, 9, 8837.	2.7	95
63	Imaging interfacial micro- and nano-bubbles by scanning transmission soft X-ray microscopy. Journal of Synchrotron Radiation, 2013, 20, 413-418.	2.4	65
64	The Morphology and Stability of Nanoscopic Gas States at Water/Solid Interfaces. ChemPhysChem, 2012, 13, 2188-2195.	2.1	20
65	The length scales for stable gas nanobubbles at liquid/solid surfaces. Soft Matter, 2010, 6, 4515.	2.7	65
66	Nanoscale Multiple Gaseous Layers on a Hydrophobic Surface. Langmuir, 2009, 25, 8860-8864.	3.5	74
67	Hollow Silica Spheres: Synthesis and Mechanical Properties. Langmuir, 2009, 25, 2711-2717.	3.5	172
68	Long lifetime of nanobubbles due to high inner density. Science in China Series G: Physics, Mechanics and Astronomy, 2008, 51, 219-224.	0.2	61
69	Photocatalytic Induction of Nanobubbles on TiO ₂ Surfaces. Journal of Physical Chemistry C, 2008, 112, 4029-4032.	3.1	27
70	INVESTIGATION ON THE MORPHOLOGY OF PRECIPITATED CHEMICALS FROM TE BUFFER ON SOLID SUBSTRATES. Surface Review and Letters, 2007, 14, 1121-1128.	1.1	6
71	Electrochemically Controlled Formation and Growth of Hydrogen Nanobubbles. Langmuir, 2006, 22, 8109-8113.	3.5	197
72	Formation of Bulk Nanobubbles Induced by Accelerated Electrons Irradiation: Dependences on Dose Rates and Doses of Irradiation. Langmuir, 0, , .	3.5	3